THE JOURNAL OF PHYSICAL CHEMISTRY C

Article

pubs.acs.org/JPCC

Functionalization of Single-Layer Nitrogene by Vacancy, Adatoms, and Molecules

Yelda Kadioglu,[†] O. Üzengi Aktürk,[‡] Ethem Aktürk,*[,¶,§] and Salim Ciraci*[,∥]

[†]Department of Physics, Adnan Menderes University, Aydın 09010, Turkey

[‡]Department of Electrical and Electronic Engineering, Adnan Menderes University, 09100 Aydın, Turkey

[¶]Department of Physics, Adnan Menderes University, Aydın 09010, Turkey

[§]Nanotechnology Application and Research Center, Adnan Menderes University, Aydın 09010, Turkey

[∥]Department of Physics, Bilkent University, Ankara 06800, Turkey

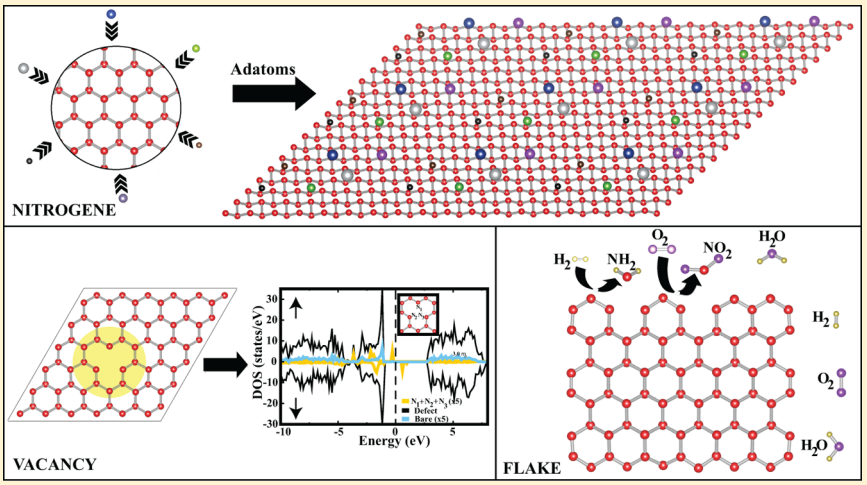

ABSTRACT: Despite its strong N_2 molecule, recent studies have shown that nitrogen, the lightest group V element, remains stable in the free-standing, single-layer buckled honeycomb structure with two-dimensional (2D) hexagonal lattice. This structure is called nitrogene and is predicted to be a nonmagnetic, wide band gap semiconductor or insulator. In this paper, we investigated the formation of a single vacancy, as well as the adsorption of selected single adatoms and molecules on 2D nitrogene, using the supercell method within the density functional theory. Through the consideration of large supercells, the couplings between adjacent vacancies and adspecies are minimized; hence, the results are taken to represent single, isolated defect and adspecies. We found that a single vacancy contributes a local magnetic moment and filled and empty localized gap states at low temperature but is prone to instability due to thermal excitations. Adatoms are bound to the surface of nitrogene and form localized gap states contributing a diversity of electronic and magnetic properties. Adsorption of adatoms, such as B, C, Si, and N, however, give rise to local and strong reconstruction in nitrogene in their close proximity. Notably, a N adatom forms a strong N_2 molecule by removing one N atom from nitrogene and leaves a vacancy behind. Conversely, the interactions between selected molecules, such as H_2, O_2, H_2O, and N_2, and the surface of nitrogene are rather weak and do not induce any change in the physical properties. However, H_2 and O_2 can be dissociated at the edges of a nitrogene flake and concomitantly can remove host N atoms to form NH_2 and NO_2 molecules. Calculated properties of adatoms adsorbed to nitrogene differ dramatically from the properties of those adsorbed to single-layer structures of other group V elements.

INTRODUCTION

Following the synthesis of very thin phosphorene and field effect transistor fabricated thereof,[1] recent theoretical studies have shown the stability of single-layer (SL), free-standing structures of group V elements or pnictogens (N, P, As, Sb, and Bi). These SL structures are nitrogene,[2,3] phosphorene,[4] arsenene,[5] antimonene,[6,7] and bismuthene.[8] Among pnictogens, nitrogen has a liquid phase at 77 K and molecular/nonmolecular solid phases[9−14] and three-dimensional (3D) cubic gauche(cg-N) crystalline phase[15,16] at extreme conditions, but normally it is gaseous at room temperature and forms the strongest molecule in nature, N_2. It was surprising that nitrogen can also form a stable, two-dimensional (2D) crystalline phase with hexagonal lattice in SL, buckled honeycomb structure termed *nitrogene*.[2] While the N_2 molecule is triple-bonded, nitrogene is constructed from single-bonded N atoms similar to

Received: November 21, 2016
Revised: February 28, 2017
Published: February 28, 2017

DOI: 10.1021/acs.jpcc.6b11705
J. Phys. Chem. C 2017, 121, 6329−6338

the 3D cg-N crystalline phase. Furthermore, it was predicted that nitrogene can remain stable above room temperature and can form stable nanoribbons, bilayers, and 3D graphitic structures named *nitrogenite*.[2] Unlike semimetallic graphene[17] or silicene[18,19] having perfect electron−hole symmetry, nitrogene is a nonmagnetic, wide band gap semiconductor or insulator. Experimentally, Harada et al. reported the epitaxial growth of 2D nitrogen atomic sheet in GaAs.[20] Also, the structure of the monolayer consisting of N_2 molecules adsorbed on MgO(100) powder was investigated at 10−60 K.[21]

In this paper we investigate single-vacancy and divacancy defects of SL nitrogene, as well as the adsorption of 13 selected single adatoms (i.e., H, Li, O, Al, P, Cl, Ti, As, Sb, B, C, Si, and N) and physisorption of 4 molecules (i.e., H_2, O_2, H_2O, and N_2). These adatoms and molecules were known to engage in chemical interactions with various SL structures, like graphene, silicene, BN, MoS_2,[22−31] antimonene,[32] and arsenene,[33] and give rise to novel functional properties. For example, Ti and Li adatoms were shown to be crucial in high-capacity hydrogen storage when adsorbed on graphene.[23,24,26] Some of these adatoms by themselves (N, C, Si, P, As, and Sb) can form free-standing, honeycomb structures with a 2D hexagonal lattice.

Our objectives in this paper are three-fold: (i) We first test whether the stability of nitrogene is maintained after the creation of point defects, such as a vacancy, and after the adsorption of single adatoms. (ii) We reveal the modification of the properties of nitrogene after the creation of vacancy and adsorption of single adatoms. In this way we explore the functionalization of nitrogene. (iii) The edges of a nitrogene flake have 2-fold coordinated N atoms behaving as active sites, which may lead to the dissociation of certain molecules. We examine the interaction of these active sites with selected molecules and explore whether a dissociative reaction can take place and lead to a hydrogen evolution process.

In this study, we found that a single vacancy can contribute a local magnetic moment of 3 μ_B and spin-polarized localized states in the gap. Adatoms, such as H, Li, O, Al, P, Cl, Ti, As, and Sb, adsorbed on the surface of 2D nitrogene can form strong bonds inducing minute or moderate local deformations in the structure of substrate and leading to diversity of electronic and magnetic properties. However, the adsorption of B, C, Si, and N results in massive local reconstruction; even a hole can be created in nitrogene. The molecules, such as H_2, O_2, H_2O, and N_2, interact weakly with the surface nitrogene. However, H_2 and O_2 form NH_2 and NO_2 molecules, respectively, upon their dissociation at the edges of a nitrogene flake.

COMPUTATIONAL DETAILS

The predictions of this study are obtained by carrying out first-principles plane wave calculations based on spin-polarized density functional theory (DFT)[34] within supercell geometry using periodic boundary conditions. A single vacancy is created or single adatom (molecule) is adsorbed at its specific equilibrium positions of each (6 × 6) supercell of nitrogene, so that a 2D regular array of vacancy or adspecies is obtained. The details of supercell geometry will be given in forthcoming sections. The Perdew−Burke−Ernzerhof functional (PBE) is used for the exchange−correlation potential in generalized gradient approximation (GGA),[35] and the PAW pseudopotentials are adopted.[36,37] In all calculations, corrections of van der Waals (vdW) interactions in the DFT-D2 level[38] are included. Different methods of the vdW corrections have been discussed in the literature.[39−41] While the DFT-D2 method overbinds by ∼8% and hence underestimates the interlayer spacing of graphite and 2h-MoS_2, the first-principles DFT-DF[41] method slightly underbinds, but is sophisticated to use.

The electron wave functions were expanded in plane waves up to a kinetic energy cutoff of 550 eV. The Brillouin zone (BZ) is sampled using a Monkhorst−Pack scheme[42] by (5 × 5 × 1) mesh in the *k*-space. The energy convergence criterion is taken as 10^{-5} eV between two successive iterations. The maximum pressure on the unit cell is reduced to less than 1 kbar. Calculations from the first principles were performed using Vienna Ab Initio Simulation Package (VASP).[43,44] Caution was taken in the optimization of systems having magnetic ground state. To this end we performed a series of total energy calculations for single vacancy in nitrogene (ntrgn +V) or single adatom adsorbed to nitrogene (ntrgn+A), each having different, fixed magnetic moment. Then the magnetic moment of the optimized structure is determined as the magnetic moment corresponding to that of the minimum total energy.

Calculation of the binding energy is crucial for the interaction of adatom or molecule with 2D nitrogene. A binding energy larger than ∼1 eV usually implies the chemisorption of adatom with the exchange of charge with nitrogene. When compared with this binding energy, the contribution of vdW interaction is minute. However, in the case of physisorption, the binding energy is weak and ranges between ∼40 and 110 meV for molecules considered in this study. In contrast to chemisorption, the contribution of vdW interaction dominates the physisorption energy. In forthcoming sections we present the contribution of vdW interaction in typical chemisorption and physisorption bonds.

The binding energy E_b, (or physisorption energy, E_a) is obtained from the expression, $E_b(E_a) = E_T[A(M)] + E_T[\text{bare} \sim \text{ntrgn}] - E_T[\text{ntrgn+A(M)}]$ in terms of the total, spin-polarized energies of the free adatom (molecule), bare nitrogene, and the system of adatom adsorbed (molecule physisorbed) to the nitrogene. Here A(M) denotes adatom (molecule). Because the initial configuration of the molecule relative to the substrate is crucial for physisorbed molecules, various orientations have been also tested to achieve the highest physisorption energy. The energy released after the formation of a new molecule NM = NH_2 or NO_2 following the dissociation of one N atom from the edge of nitrogene and the dissociation of molecule M = H_2 or O_2 at the edge of the nitrogene flake is calculated $E_f = E_T[\text{bare} \sim \text{ntrgn}] + E_T[M] - E_T[\text{ntrgn+NM}]$, where $E_T[\text{ntrgn +NM}]$ is the optimized total energy of the flake with one N atom removed from edge plus the new molecule formed in the process. This energy corresponds to the formation energy of the new molecule, NM, at $T = 0$ K. We note that in this study the calculated positive values of E_b, E_a, cohesive energy E_C, and formation energy E_f indicate that the process under study is favorable energetically.

The formation energy of a single vacancy is obtained from $E_v = E_T[\text{ntrgn+}V] - \frac{m-1}{m}E_T[\text{bare} \sim \text{ntrgn}]$[45] in terms of the total energy of the cell containing a vacancy and of bare nitrogene. Here m is the number of atoms in the SL nitrogene. The stability of the single vacancy in nitrogene has been tested by performing finite temperature ab initio molecular dynamics (MD) calculations with time steps of 2 fs. We performed MD simulations using Nosé thermostat for the duration of 2 ps at

DOI: 10.1021/acs.jpcc.6b11705
J. Phys. Chem. C 2017, 121, 6329−6338

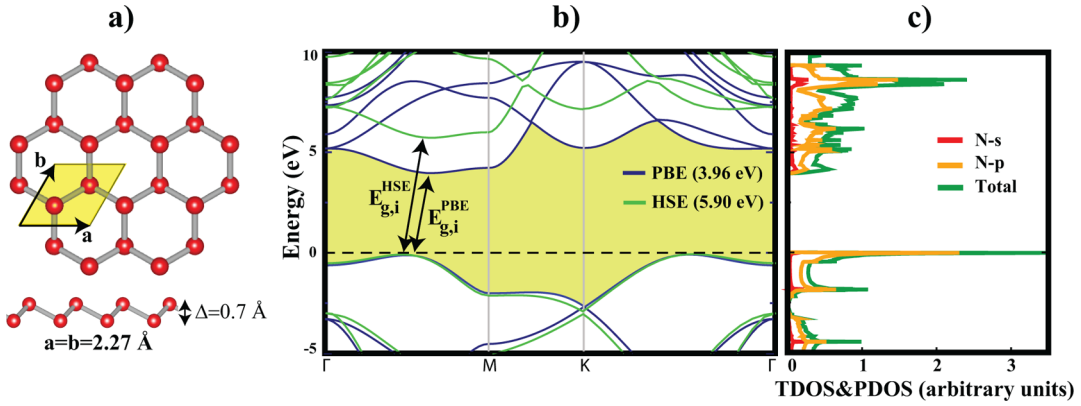

Figure 1. Free standing SL nitrogene: (a) top and side views of buckled honeycomb structure. The primitive unit cell of the 2D hexagonal lattice is shaded, and lattice constants **a** and **b** are indicated. (b) Electronic energy band structure calculated using PBE and HSE (see text). The fundamental band gap calculated by PBE is shaded. (c) Total and s- and p-orbital projected density of states, TDOS and PDOS, respectively. The zero of energy is set at the top of the valence band.

different constant temperature levels, where the velocities were normalized after each 40 time steps.

NITROGENE

That nitrogen atoms form 2D single-layer, stable, wide band gap semiconductor (or insulator) with hexagonal lattice was first predicted by Özçelik et al.[2] For the sake of completeness, part of their results relevant to the present study is reproduced here. We start with reproducing the atomic and electronic structure of nitrogene, because it is essential in the analysis of its interaction with adatoms and molecules.

The cohesive energy of the structure optimized nitrogene is E_C = 3.67 eV. The atomic configuration and primitive cells of nitrogene in buckled honeycomb structure is shown in Figure 1a together with the lattice constants of its 2D hexagonal lattice. Because of buckling, nitrogene consists of two atomic planes of nitrogen atoms, which are separated by 0.7 Å. The electronic energy band structure of bare nitrogene calculated by PBE is presented in Figure 1b. Accordingly, nitrogene is a wide band gap semiconductor with an indirect band gap of $E_{g,i}$ = 3.96 eV occurring between conduction and valence band along the Γ−*M* direction of BZ. This band gap increases to $E_{g,i}$ = 5.90 eV after the HSE06 correction.[46,47] The total and s- and p-orbital projected densities of states presented in Figure 1c indicates that the edges of valence and conduction band are composed of predominantly p-orbitals.

SINGLE VACANCY

Single vacancy in nitrogene, i.e., ntrgn+V, is created by removing one N atom from each (6 × 6) supercell of the buckled honeycomb structure and subsequently by optimizing the defected structure. In this process, the vacancy formation energy is calculated to be E_v = 1.19 eV. Through the uncompensated spins of missing nitrogen atom, ntrgn+V attains a permanent magnetic moment of 3 μ_B at the vacancy site. We note that the earlier calculation,[2] which predicted the formation energy of a single vacancy as 5.90 eV, used a formal definition which is different from that in the present study.

The effect of the vacancy on the electronic structure is analyzed using density of states. In Figure 2, the calculated spin-polarized densities of states of ntrgn+V are presented. A single vacancy gives rise to spin-polarized states in the fundamental band gap. These states are localized at the vacancy site, in

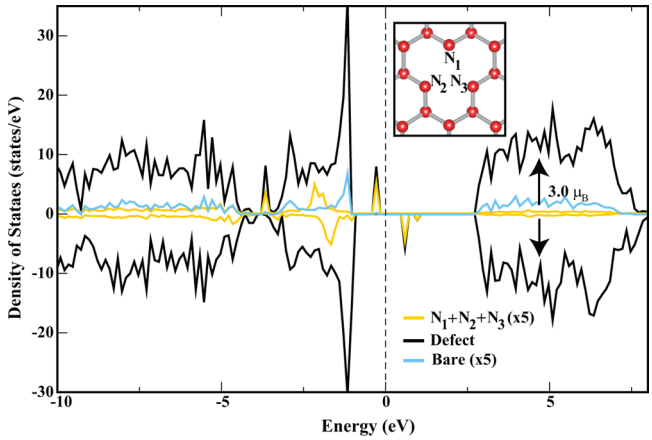

Figure 2. Spin-polarized density of states of nitrogene with a single vacancy, i.e., ntrgn+V. Atomic structure of the vacancy and three 2-fold coordinated N atoms, N_1, N_2, and N_3, are shown in the inset. The sum of local density of states on three N atoms surrounding the vacancy (yellow lines) and the local density of states on a host N atom of nitrogene farthest from the vacancy (light blue lines) are also presented. The latter local density of states represents the total density of states of "bare" and extended nitrogene. The zero of energy is set to the Fermi level of ntrgn+V.

particular at N atoms surrounding the vacancy. In addition, resonance states due to the vacancy can occur in the band continua. The energy shifts of vacancy-induced localized states relative to the "bare" and extended nitrogene having single vacancy can be retrieved by calculating the local density of states (LDOS) at a host N atom in the supercell, which is farthest from the vacancy. This state density is specified in Figure 2 as bare nitrogene. In the band gap, localized spin up states due to the vacancy are filled, while localized spin down states are empty; the gap between them is 0.5 eV. Apparently, this situation indicates a dramatic effect of vacancy, whereby the wide band gap of bare nitrogene is reduced to a narrow band gap.

Based on finite temperature, ab initio MD calculations in the temperature range between 0 and 500 K, the single vacancy in nitrogene is found to be stable at 0 K, but it is prone to severe deformations under thermal excitations at and above 300 K. These results imply that the single vacancy can remain stable at low temperature; however, instabilities can occur at room

DOI: 10.1021/acs.jpcc.6b11705
J. Phys. Chem. C 2017, 121, 6329−6338

temperature and above. Similar calculations resulted in the structural instability of divacancy in nitrogene.

■ ADSORPTION OF ADATOMS

In our study of the adsorption of adatoms (H, Li, O, Al, P, Cl, Ti, As, Sb, B, C, Si, and N) to nitrogene, we first determine the equilibrium site (or geometry) by the optimization of the atomic structure of adatom and nitrogene underneath. Using the optimized atomic structure corresponding to the equilibrium geometry, we calculate electronic and magnetic structure together with the adatom-induced localized states. In this way we reveal the functionalization of nitrogene through modifications of its electronic and magnetic properties.

Optimized Structure and Energetics of Adsorbed Adatoms. In Figure 3 we describe our models of supercells of

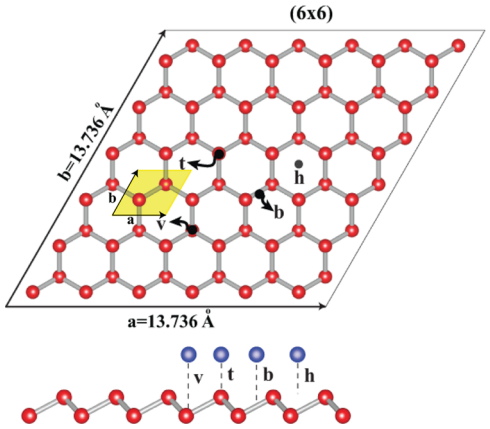

Figure 3. Top and side views of the atomic configuration of the (6 × 6) supercell of nitrogene, which is used to treat single vacancy, adsorbed adatoms, and physisorbed molecules. The 2D hexagonal primitive unit cell of nitrogene is delineated and shaded. Possible adsorption sites are the top site (t), where the adatom is on top of a host N atom; the bridge site (b), where the adatom is above the center of the N−N bond; the hollow site (h), where the adatom is located above the center of hexagons of the host N atoms; and the valley site (v), where the adatom is placed on top the low-buckled host N atom. Host N atom and adatom are represented by red and blue balls, respectively. Optimized lattice constants of the supercell are $a = b =$ 13.736 Å.

2D nitrogene showing possible sites of adsorption or physisorption [such as top (t), bridge (b), hollow (h), and valley (v) sites] above the substrate plane. The supercells are constructed from a (6 × 6) supercell comprising 36 primitive cells of 2D nitrogene, which is found to give rise to negligible coupling between adjacent adatoms. The minimum energy adsorption site corresponding to the equilibrium structure of an adatom (molecule) together with the atomic configuration of the underlying nitrogene is determined through a comprehensive optimization process. To this end, each adatom or molecule is placed to all possible sites described in Figure 3 at a distant height from nitrogene. Subsequently, all atomic positions including the height of the adatom or molecule and atomic positions of substrate atoms are relaxed to attain the minimum total energy, E_T[ntrgn+A(M)] and minimum forces on each atom. The site yielding the minimum value among the total energies calculated for a particular adatom is taken as the equilibrium adsorption site of this adatom. It should be noted that contrary to the case of the large supercell in this study, adatoms treated using small supercells lead to high coverage, namely $\Theta \sim 1$, and result in specific decorations of nitrogene. Under these circumstances, the coupling among adsorbed adatoms increases, and at the same time the interaction between an adatom and substrate can be modified. At the end, the physical properties of the adatom overlayer and of nitrogene can be modified significantly depending on the coverage. In particular, the localized electronic states originated from adatoms can form energy bands at high coverage. In the present situation using (6× 6) supercells, small adatom−adatom coupling lets us interpret our results as if they correspond to isolated single adatom adsorption (or dilute doping).

All adatoms treated in this paper form chemical bonds with nitrogene. For adatoms H, Li, O, Al, P, Cl, Ti, As and Sb, only local deformations of nitrogene at the proximity of adsorbate have occurred, but overall honeycomb geometry has been retained. However, the adsorption of adatoms B, C, and N in the first row, as well as Si gives rise to local reconstruction in nitrogene followed by bond breaking, even dissociation of the host N atoms. We therefore examine the adsorption of adatoms in two categories.

In the first category, the equilibrium adsorption geometries of H, Li, O, Al, P, Cl, Ti, As, and Sb are presented in Figure 4. The hydrogen atom is adsorbed to t-site with a binding energy of 2.09 eV and contribute a local magnetic moment of 1.0 μ_B. The van der Waals contribution to the binding energy is a small

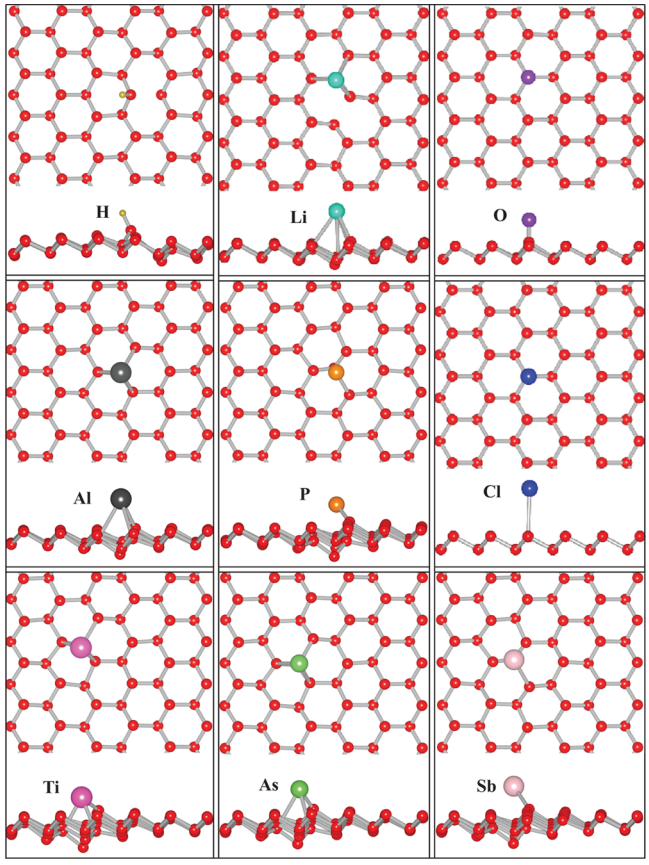

Figure 4. Top and side views of the equilibrium atomic configuration of the adatoms H, Li, O, Al, P, Cl, Ti, As, and Sb adsorbed to nitrogene. Despite deformations at the close proximity of adatoms, the overall honeycomb geometry of nitrogene is retained. Host N atoms of nitrogene are described by small, red balls.

DOI: 10.1021/acs.jpcc.6b11705
J. Phys. Chem. C 2017, 121, 6329−6338

fraction of the binding energy and is only 90 meV. Lithium prefers to v-site and forms a strong bond with binding energy of 2.51 eV and local magnetic moment of 1.0 μ_B. Oxygen at t-site forms even stronger bonds with host N atom. Group V elements or pnictogens, P, As, and Sb atoms can be viewed as a subgroup; they are adsorbed at a t-site but slightly shifted toward v-sites and form bonds with binding energies ranging from ∼1.1 to 1.5 eV with 1.0 μ_B local magnetic moment. Chlorine at t-site forms a weak bond with a binding energy of 0.51 eV at the t-site. In contrast, Ti at a v-site forms a strong bond and causes local deformation and higher local magnetic moment of 2.0 μ_B. Calculated binding energies and relevant structural parameters and local magnetic moments related to these adatoms are presented in Table 1.

Table 1. Values Calculated for the Adsorption Adatoms H, Li, O, Al, P, Cl, Ti, As, and Sb to Nitrogene[a]

adatom (A)	site	E_b (eV)	h (Å)	d_{A-N} (Å)	μ (μ_B)
H	t	2.09	1.72	1.04	1.0
Li	v	2.51	1.65	1.97	1.0
O	t	3.24	1.43	1.20	0.0
Al	v	2.29	1.65	2.23	1.0
P	v-b	1.46	1.13	1.69	1.0
Cl	t	0.51	2.52	2.56	1.0
Ti	v	4.76	1.10	1.98	2.0
As	v	1.13	1.48	1.87	1.0
Sb	v	1.30	1.65	2.09	1.0

[a]Adsorption site; binding energy, E_b; height (distance) of the adatom from the original, high-lying N atomic plane of nitrogene, h; the smallest distance between the adatom and host N atom of nitrogene, d_{A-N}; the local magnetic moment, μ.

As shown in Figure 5, B adatom in the second category causes massive local reconstruction in nitrogene at the close proximity of adsorption site. N−N bonds are broken to form a B−N−N atomic string; hence, a hexagon is destroyed to open a hole in nitrogene. The bonding is strong with the binding energy of 5.67 eV and local magnetic moment of 1 μ_B. Carbon and silicon adatoms cause similar effects in nitrogene with binding energies 5.11 and 5.69 eV, respectively. A nitrogen atom forms a N_2 molecule by removing one N atom of nitrogene and leaves the substrate by creating a single vacancy behind. Calculated values regarding these adatoms are presented in Table 2.

Electronic and Magnetic Properties. Our main objective in the doping of nitrogene is to modify its electronic and magnetic properties and hence to make it more functional. Adsorbed adatoms can modify the electronic and magnetic structure of nitrogene locally. In the doping at very low coverage, single adsorbed or substituted foreign atoms give rise to localized states in the fundamental band gap and/or resonance states in the band continua.

The present analysis uses a scheme to deduce the effects of adsorption, in particular, energy shifts of adatom induced localized states relative to the "bare" extended substrate (ntrgn). Here, the total and adatom projected densities of states are examined to reveal the energy locations of dopant states relative to the fundamental band gap of the bare extended substrate, as shown in Figure 6. The density of states of the bare extended substrate and the energy position of its fundamental band gap is retrieved from the local density of states, LDOS, calculated at a N host atom, which is farthest

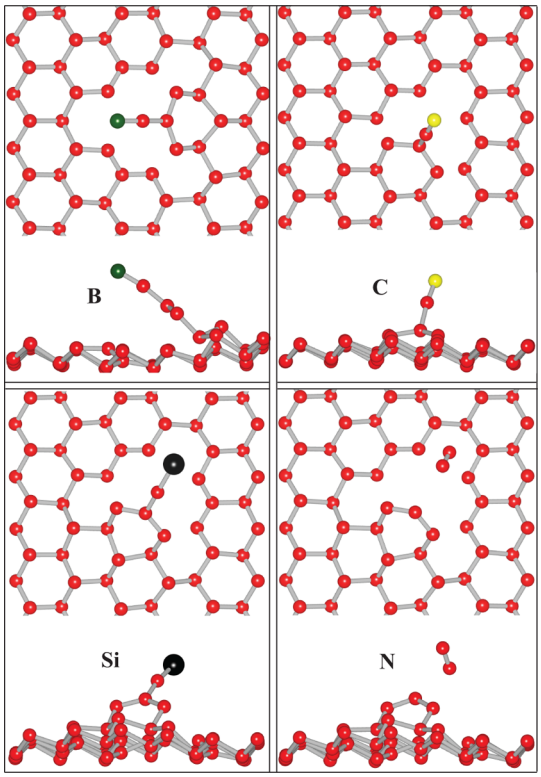

Figure 5. Top and side views of the equilibrium atomic configuration of the adatoms B, C, Si, and N adsorbed to nitrogene. Upon adsorption, massive reconstruction and/or dissociation have occurred by destroying one hexagon of the substrate and creating a single vacancy. Host N atoms of nitrogene are described by small, red balls.

Table 2. Calculated Values of Adatoms B, C, Si, and N Adsorbed to Nitrogene[a]

adatom (A)	E_b (eV)	h (Å)	d_{A-N} (Å)	μ (μ_B)
B	5.67	3.07	1.25	1.0
C	5.11	2.88	1.19	2.0
Si	5.69	3.33	1.58	0.0
N	8.22	4.14	3.29	1.0

[a]Binding energy, E_b; height (distance) of the adatom from the original, high-lying N atomic plane of nitrogene, h; the smallest distance between the adatom and N host atom of nitrogene, d_{A-N}; the local magnetic moment, μ.

from the adatom in the supercell. This way, the energy positions of adatom-induced localized states can be determined relative to the band edges of the bare extended substrate with reasonable accuracy. The common Fermi level at T = 0 K (also the zero of energy), that is, the energy level separating the filled states from the empty states of ntrgn+A system, is normally within the fundamental band gap; it can move toward the band edges depending on the character of the localized states. Notably, for the systems containing very dilute adatoms or dopants, the Fermi level has to be determined through the chemical potential of the Fermi−Dirac distribution. We note that because of the finite size of the supercell the coupling between farthest host N atom and a few specific adatoms can give rise to small uncertainties in the exact position of band edges. Nevertheless, these uncertainties do not affect our discussion here.

States derived from a hydrogen adatom adsorbed to nitrogene are spin-polarized and appear in the gap near the

DOI: 10.1021/acs.jpcc.6b11705
J. Phys. Chem. C 2017, 121, 6329−6338

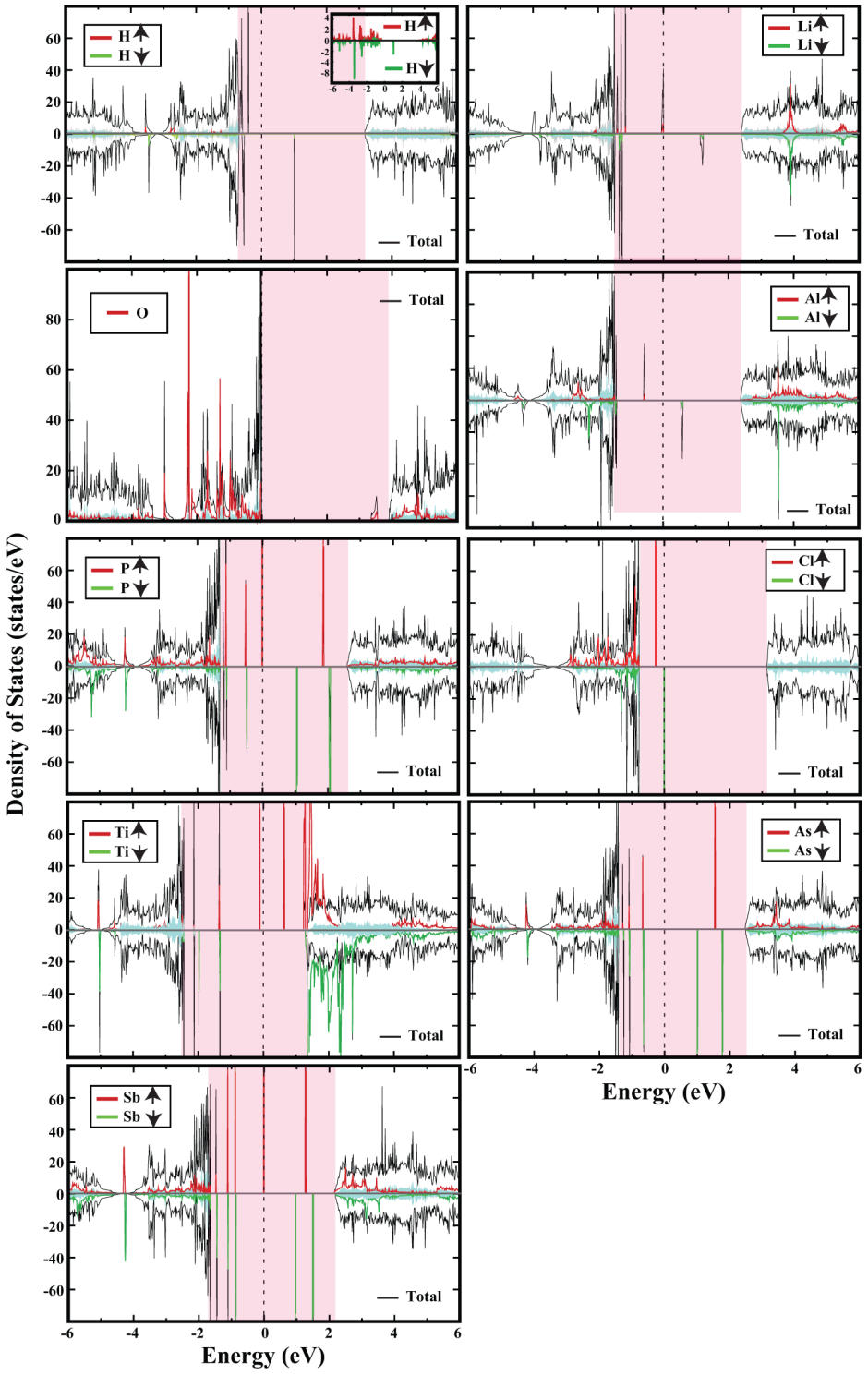

Figure 6. Densities of states calculated for an adatom adsorbed to each (6 × 6) supercell of nitrogen at equilibrium sites. Total density of states (TDOS) is shown by thin black lines. The density of states of the "bare" extended nitrogene substrate is obtained by projecting TDOS on a host N atom farthest from the adatom and is shown by light blue tone; its band gap is shown by the pink zone. Red and green lines indicate the densities of spin up and spin down states of TDOS projected to the adatom, respectively. The zero of the energy is set at the common Fermi level shown by the dashed vertical line. For clarity, the projected densities of states of H is shown in the inset.

edge of the valence band. Normally, Li adatom is used to donate part of its valence electrons to the conduction band states of the substrate, when the fundamental band gap is not wide. Here, Li-derived spin up localized states occur ∼1.2 eV above the edge of the valence band of nitrogene. They are filled and set the Fermi level. The empty spin down states occur also in the gap 1 eV above the Fermi level. The oxygen adatom forms strong bonds; hence, resonance states originating from O overlap with the valence band of bare nitrogene. Empty localized states are found in the gap, below the conduction band edge. States originating from Al are spin-polarized; localized, filled spin up and empty spin down states are found

DOI: 10.1021/acs.jpcc.6b11705
J. Phys. Chem. C 2017, 121, 6329−6338

in the gap. The localized, spin-polarized states originating from P, Cl, As, and Sb in the band gap of bare nitrogene share similar characters. Being a transition-metal atom, Ti exhibits differences with several localized and spin-polarized gap states leading to local magnetic moment relatively higher than others.

The local deformations resulted from the adsorption of the adatoms B, C, Si and N give rise to metastable atomic structures, which may undergo changes. Accordingly, the electronic properties of these metastable structures may not be uniquely determined.

PHYSISORPTION OF MOLECULES ON NITROGENE

Four molecules, H_2, O_2, H_2O, and N_2, are attached to the surface of 2D nitrogene through weak and attractive vdW interaction; they do not engage in significant chemical interactions with nitrogene. Accordingly, the binding of these molecules are specified as physisorption, and associated energies are small. The physisorption of these four molecules are investigated by placing them in their different possible configurations above various sites in Figure 3 at large distances. Then the atomic positions of the whole system, namely, molecule and substrate atoms, are optimized to attain the minimum total energy as well as atomic forces. The optimized structures corresponding to minimum total energy are presented in Figure 7. Calculated values of physisorption energies, E_a, and molecule−substrate distances h and d are listed in Table 3.

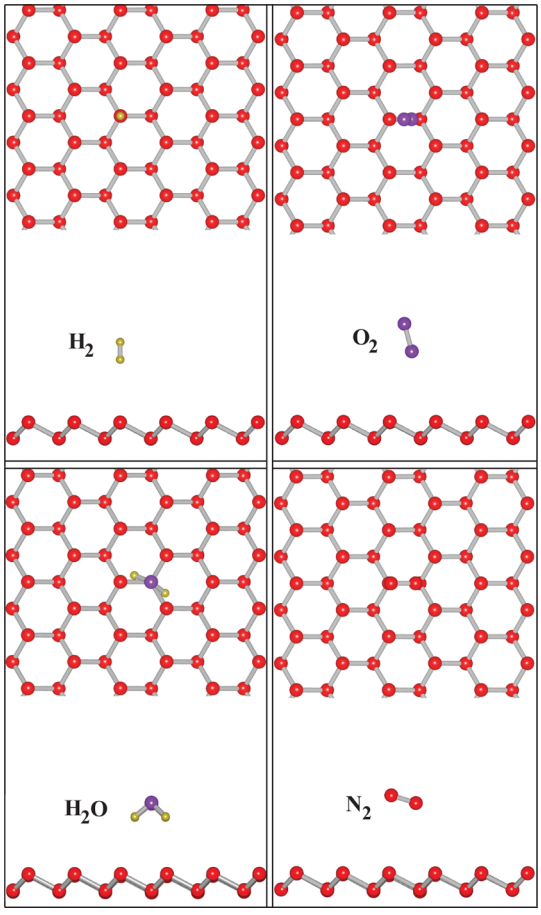

Figure 7. Top and side views of the equilibrium atomic configuration of the molecules H_2, O_2, H_2O, and N_2 physisorbed to nitrogene.

Table 3. Calculated Equilibrium Physisorption Energy, E_a; Height from the Original Atomic Plane of Nitrogene, h; Minimum Distance between Host N Atom and the Molecule (M) Physisorbed to Nitrogene

molecule (M)	E_a (meV)	h (Å)	d_{M-N} (Å)
H_2	40	2.71	2.73
O_2	50	3.02	3.18
H_2O	110	2.47	2.60
N_2	50	3.02	3.31

The calculated binding (physisorption) energies are small and range between 40 and 110 meV. To test the contribution of vdW interaction to the binding, we calculated the binding energy of H_2O without vdW interaction. We found $E_a = -8$ meV. Even if this small energy marks the accuracy limits of DFT calculations, the interaction between H_2O and nitrogene is nonbonding without vdW interaction. In compliance with weak binding, the distances between molecules and nitrogene substrate are rather large. Accordingly, nitrogene is rather inert to H_2, O_2, H_2O, and N_2 molecules. Apparently, the electronic properties of nitrogene cannot be affected through the physisorption of these molecules.

Dissociation of Molecules at the Edges of Nitrogene. It was shown that edges of flakes, vacancy defects, or specific adatoms adsorbed to graphene or MoS_2 constitute active sites, where dissociations of molecules, like H_2, O_2, and H_2O, can be mediated.[30,48] In this section, we investigate the interaction of the edge of nitrogene with H_2, O_2, and H_2O. Our objective is to see whether the dissociations of these molecules are realized at the edges. We used the supercell geometry consisting of rectangular nitrogene flakes and vacuum space separating each flake from its neighbors. Nitrogen atoms at the zigzag and armchair edges of the flake are 2-fold coordinated and hence can act as chemically active sites.

The dissociation of molecules at the edges of the nitrogene flake in the present study is a complex process and depends on several conditions and parameters, such as the initial distance between molecule and N atom at the edge, the orientation of the molecule relative to the edge, the angle of approach, etc. In principle, molecules are usually dissociated if they become very close to the edges of the flake. Here, using only limited number of test simulations, we show that H_2 and O_2 molecules interacting with the specific edges of the nitrogene flake can dissociate into their constituent atoms under specific circumstances. Concomitantly, the nearest 2-fold coordinated N atom is removed from the edge, and eventually new molecules, NH_2 and NO_2, are formed. This process can occur with positive formation energy even at $T = 0$ K either spontaneously or by overcoming a potential barrier.

In Figure 8, one sees that H_2, O_2, and H_2O molecules are situated near the zigzag, armchair edges of nitrogene flake. When H_2 is placed perpendicularly at a distance of 1.05−1.20 Å from the zigzag edge, it goes away in the course of structure optimization and eventually is physisorbed at a distance of 2.73 Å. The similar situation also occurs when H_2 is placed parallel to the zigzag edge facing a 2-fold coordinated host N atom. Upon structure optimization, it goes away and is physisorbed at a distance of 3.11 Å. However, H_2 is dissociated when it approaches the host N atom parallel to the edge as close as 1.02 Å. Concomitantly, a host N atom from the edge is removed and is implemented to form NH_2 molecule. Using the expression presented in Computational Details, the formation energy at T

DOI: 10.1021/acs.jpcc.6b11705
J. Phys. Chem. C 2017, 121, 6329−6338

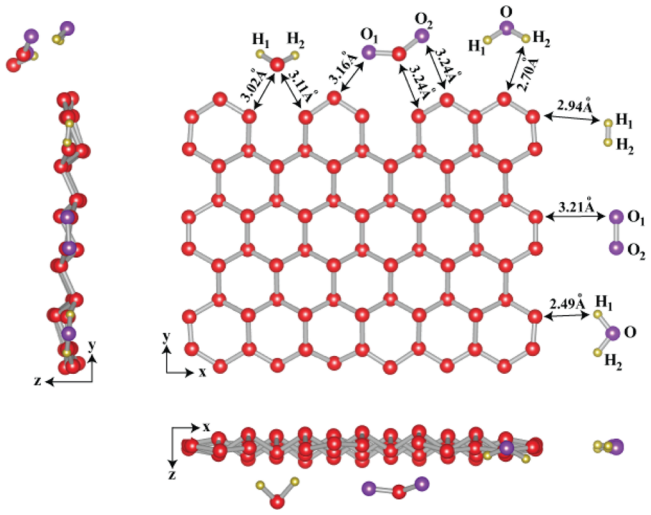

Figure 8. Top and two side views of the atomic configurations of H_2, O_2, and H_2O molecules interacting with the zigzag and armchair edges of a rectangular nitrogene flake. At the zigzag edge, 2-fold coordinated N atoms are implemented to dissociated H_2 and O_2 molecules to form eventually NH_2 and NO_2 molecules. H_2O remains intact at both edges.

= 0 K is calculated to be E_f = 1.17 eV, indicating that this process is exothermic and hence is favorable energetically. Alternatively, the formation energy E_f at T = 0 K can be calculated as 1.19 eV using the expression $E_f = 2E_T[\text{H atom}] + E_T[\text{N atom}] + E_C[H_2] + E_d[\text{N}] - E_T[NH_2]$, in terms of free atom total energies, the cohesive energy of H_2 molecule $E_C[H_2]$, the energy needed to remove a 2-fold N atom from the edge of the flake $E_d[\text{N}]$, and the total energy of NH_2 molecule. The energy $E_d[N]$ is estimated as $E_d[N] = 2E_C[\text{ntrgn}]/3$ from the cohesive energy of nitrogene. Our simulation of the formation of NH_2 following the dissociation of H_2 and N atom from the edge indicates that there exists a barrier between flake and H_2 molecule at about ∼1.03 Å. Once this barrier is overcame, NH_2 can form spontaneously.

As for O_2, it goes away from the edge if it is placed parallel to the edge at a distance of 1.85 Å. However, dissociation of O_2 and subsequently the formation of NO_2 can take place spontaneously if an O_2 molecule approaches parallel to the edge as close as 1.50 Å. The formation energy is calculated to be E_f = 2.91 eV. In terms of constituent free atom energies, cohesive energy of O_2, and the dissociation energy of 2-fold N atom from the edge of the flake E_d, the formation energy of NO_2 molecule is estimated to be 2.95 eV; hence, it is exothermic and is favorable energetically.

The armchair edge of nitrogene appears to be less active than the zigzag edge; if H_2 and O_2 molecules are placed parallel to this edge at the same distances as in the case of the zigzag edge, both molecules go away and attain equilibrium binding at ∼2.75 and ∼3.10 Å from the edge. However, if they approach with an angle of 30° with the normal, the dissociation can occur spontaneously at appropriate distance from the edge N atoms. Contrary to H_2 and O_2, H_2O remains intact as a molecule, even if it is placed close to the edges. Results of our simulation study related with the dissociation of specific molecules can be summarized as follows: (i) Because 2-fold coordinated N atoms at the zigzag and armchair edges of a nitrogene flake are chemically active and they can mediate dissociation of specific molecules, they deserve further attention. (ii) Depending on its orientation and distance from the host N atoms, H_2 and O_2 molecules can dissociate spontaneously and concomitantly can form NH_2 and NO_2 molecules. (iii) As compared to H_2 and O_2 molecules, H_2O molecule is relatively robust against dissociation at the edges of nitrogene.

CONCLUSIONS

We presented the analysis of the formation of a single vacancy as well as the interaction between selected single adatoms and molecules with nitrogene, a 2D single-layer buckled honeycomb structure of the lightest atom in group V family.

Upon formation of a vacancy, localized, filled, spin up states and empty spin down states occur in the fundamental band gap and a local permanent magnetic moment of 3 μ_B is attained. However, structural instabilities can be induced by thermal excitations at room temperature.

Selected adatoms can form rather strong bonds at the surface of 2D nitrogene by exchanging electronic charges and give rise to local deformations. The honeycomb structure is maintained despite the local deformations induced by the adsorption of adatoms like H, Li, O, Al, P, Cl, Ti, As, and Sb. However, upon the adsorption of adatoms, B, C, Si, and N massive local deformations involving also bond breaking can occur; even a hole can form. For example, a N adatom approaching the surface of nitrogene surface can remove one host N atom and form N_2 molecule leaving behind a vacancy. The binding energies of adatoms are in the range of 1.1−5.7 eV. The chlorine adatom is an exception with binding energy smaller than 1 eV.

The adsorbed adatoms in dilute coverage can give rise to localized states in the fundamental band gap and resonance states in the band continua. In this way, the electronic structure near the band gap is modified. Most of the adatoms treated in this paper acquire local magnetic moments through their spin-polarized electronic states even though nitrogene is a nonmagnetic semiconductor.

Molecules like H_2, O_2, H_2O, and N_2 interact weakly with the surface of 2D nitrogene, and they are physisorbed to it through vdW interaction. Physical properties of nitrogene cannot be affected from the physisorption of these molecules. However, when placed at appropriate configuration and distance, H_2 and O_2 molecules are dissociated at the edge of a nitrogene flake, and concomitantly they form NH_2 and NO_2 molecules by removing host N atoms from the edge. In conclusion, vacancy and selected adatoms adsorbed to nitrogene surface contribute a diversity of electronic and magnetic properties, attaining functional properties. Some adatoms bring about instability upon adsorption.

AUTHOR INFORMATION

Corresponding Authors

*E-mail: ethem.akturk@adu.edu.tr. Phone: +902562130835-1894. Fax: +902562135379.

*E-mail: ciraci@fen.bilkent.edu.tr. Phone: +903122901216. Fax: +903122664579.

ORCID

Ethem Aktürk: 0000-0002-1615-7841

Notes

The authors declare no competing financial interest.

ACKNOWLEDGMENTS

The computational resources are provided by TUBITAK ULAKBIM, High Performance and Grid Computing Center

DOI: 10.1021/acs.jpcc.6b11705
J. Phys. Chem. C 2017, 121, 6329−6338

(TR-Grid e-Infrastructure). S.C. acknowledges financial support from the Academy of Sciences of Turkey (TÜBA). This research was supported by Research Fund of the Adnan Menderes University under Project No. MF-16004.

REFERENCES

(1) Li, L.; Yu, Y.; Ye, G. J.; Ge, Q.; Ou, X.; Wu, H.; Feng, D.; Chen, X. H.; Zhang, Y. Black Phosphorus Field-Effect Transistors. *Nat. Nanotechnol.* **2014**, *9*, 372−377.
(2) Özçelik, V. O.; Aktürk, O. Ü; Durgun, E.; Ciraci, S. Prediction of a Two-Dimensional Crystalline Structure of Nitrogen Atoms. *Phys. Rev. B: Condens. Matter Mater. Phys.* **2015**, *92*, 125420.
(3) Lee, J.; Tian, W.-C.; Wang, W.-L.; Yao, D.-X. Two-Dimensional Pnictogen Honeycomb Lattice: Structure,On-site Spin-Orbit Coupling and Spin Polarization. *Sci. Rep.* **2015**, *5*, 11512.
(4) Zhu, Z.; Tománek, D. Semiconducting Layered Blue Phosphorus: A Computational Study. *Phys. Rev. Lett.* **2014**, *112*, 176802.
(5) Kamal, C.; Ezawa, M. Arsenene: Two-Dimensional Buckled and Puckered Honeycomb Arsenic Systems. *Phys. Rev. B: Condens. Matter Mater. Phys.* **2015**, *91*, 085423.
(6) Aktürk, O. Ü.; Özçelik, V. O.; Ciraci, S. Single-Layer Crystalline Phases of Antimony: Antimonenes. *Phys. Rev. B: Condens. Matter Mater. Phys.* **2015**, *91*, 235446.
(7) Zhang, S.; Yan, Z.; Li, Y.; Chen, Z.; Zeng, H. Atomically Thin Arsenene and Antimonene: Semimetal-Semiconductor and Indirect-Direct Band-Gap Transitions. *Angew. Chem., Int. Ed.* **2015**, *54*, 3112−3115.
(8) Aktürk, E.; Aktürk, O. Ü.; Ciraci, S. Single and Bilayer Bismuthene: Stability at High Temperature and Mechanical and Electronic Properties. *Phys. Rev. B: Condens. Matter Mater. Phys.* **2016**, *94*, 014115.
(9) Mills, R. L.; Schuch, A. F. Crystal Structure of Gamma Nitrogen. *Phys. Rev. Lett.* **1969**, *23*, 1154−1156.
(10) Nellis, W. J.; Holmes, N. C.; Mitchell, A. C.; van Thiel, M. Phase Transition in Fluid Nitrogen at High Densities and Temperatures. *Phys. Rev. Lett.* **1984**, *53*, 1661−1664.
(11) McMahan, A. K.; LeSar, R. Pressure Dissociation of Solid Nitrogen under 1 Mbar. *Phys. Rev. Lett.* **1985**, *54*, 1929−1932.
(12) Mailhiot, C.; Yang, L. H.; McMahan, A. K. Polymeric nitrogen. *Phys. Rev. B: Condens. Matter Mater. Phys.* **1992**, *46*, 14419−14435.
(13) Mitas, L.; Martin, R. M. Quantum Monte Carlo of nitrogen: Atom, Dimer, Atomic, and Molecular Solids. *Phys. Rev. Lett.* **1994**, *72*, 2438−2441.
(14) Gregoryanz, E.; Goncharov, A. F.; Hemley, R. J.; Mao, H.; Somayazulu, M.; Shen, G. Raman, Infrared, and X-ray Evidence for New Phases of Nitrogen at High Pressures and Temperatures. *Phys. Rev. B: Condens. Matter Mater. Phys.* **2002**, *66*, 224108.
(15) Eremets, M. I.; Hemley, R. J.; Mao, H.; Gregoryanz, E. Semiconducting Non-Molecular Nitrogen up to 240 GPa and Its Low-Pressure Stability. *Nature* **2001**, *411*, 170−174.
(16) Eremets, M. I.; Gavriliuk, A. G.; Trojan, I. A.; Dzivenko, D. A.; Boehler, R. Single-bonded Cubic Form of Nitrogen. *Nat. Mater.* **2004**, *3*, 558−563.
(17) Novoselov, K. S.; Geim, A. K.; Morozov, S. V.; Jiang, D.; Zhang, Y.; Dubonos, S. V.; Grigorieva, I. V.; Firsov, A. A. Electric Field Effect in Atomically Thin Carbon Films. *Science* **2004**, *306*, 666−669.
(18) Durgun, E.; Tongay, S.; Ciraci, S. Silicon and III-V Compound Nanotubes: Structural and Electronic Properties. *Phys. Rev. B: Condens. Matter Mater. Phys.* **2005**, *72*, 075420.
(19) Cahangirov, S.; Topsakal, M.; Aktürk, E.; Şahin, H.; Ciraci, S. Two- and One-Dimensional Honeycomb Structures of Silicon and Germanium. *Phys. Rev. Lett.* **2009**, *102*, 236804.
(20) Harada, Y.; Yamamoto, M.; Baba, T.; Kita, T. Epitaxial Two-dimensional Nitrogen Atomic Sheet in GaAs. *Appl. Phys. Lett.* **2014**, *104*, 041907.
(21) Trabelsi, M.; Coulomb, J. P.; Degenhardt, D.; Lauter, H. Structures of the Nitrogen Monolayer Adsorbed on MgO(111). *Surf. Sci.* **1997**, *377-379*, 38−44.
(22) Chan, K. T.; Neaton, J. B.; Cohen, M. L. First-Principles Study of Metal Adatom Adsorption on Graphene. *Phys. Rev. B: Condens. Matter Mater. Phys.* **2008**, *77*, 235430.
(23) Yildirim, T.; Ciraci, S. Titanium-Decorated Carbon Nanotubes as a Potential High-Capacity Hydrogen Storage Medium. *Phys. Rev. Lett.* **2005**, *94*, 175501.
(24) Ataca, C.; Aktürk, E.; Ciraci, S.; Ustunel, H. High-Capacity Hydrogen Storage by Metallized Graphene. *Appl. Phys. Lett.* **2008**, *93*, 043123.
(25) Sevinçli, H.; Topsakal, M.; Durgun, E.; Ciraci, S. Electronic and Magnetic Properties of 3D Transition-Metal Atom Adsorbed Graphene and Graphene Nanoribbons. *Phys. Rev. B: Condens. Matter Mater. Phys.* **2008**, *77*, 195434.
(26) Durgun, E.; Ciraci, S.; Yildirim, T. Functionalization of Carbon-Based Nanostructures with Light Transition-Metal Atoms for Hydrogen Storage. *Phys. Rev. B: Condens. Matter Mater. Phys.* **2008**, *77*, 085405.
(27) Şahin, H.; Ciraci, S. Chlorine Adsorption on Graphene: Chlorographene. *J. Phys. Chem. C* **2012**, *116*, 24075−24083.
(28) Topsakal, M.; Gürel, H. H.; Ciraci, S. Effects of Charging and Electric Field on Graphene Oxide. *J. Phys. Chem. C* **2013**, *117*, 5943−5952.
(29) Gürel, H. H.; Ciraci, S. Enhanced Reduction of Graphene Oxide by Means of Charging and Electric Fields Applied to Hydroxyl Groups. *J. Phys.: Condens. Matter* **2013**, *25*, 435304.
(30) Ataca, C.; Ciraci, S. Dissociation of H_2O at the Vacancies of Single-Layer MoS_2. *Phys. Rev. B: Condens. Matter Mater. Phys.* **2012**, *85*, 195410.
(31) Ersan, F.; Gökoğlu, G.; Aktürk, E. Adsorption and Diffusion of Lithium on Monolayer Transition Metal Dichalcogenides ($MoS_{2(1-x)}Se_x$) Alloys. *J. Phys. Chem. C* **2015**, *119*, 28648−28653.
(32) Uzengi Akturk, O.; Akturk, E.; Ciraci, S. Effects of adatoms and physisorbed molecules on the physical properties of antimonene. *Phys. Rev. B: Condens. Matter Mater. Phys.* **2016**, *93*, 035450.
(33) Ersan, F.; Akturk, E.; Ciraci, S. Interaction of Adatoms and Molecules with Single-Layer Arsenene Phases. *J. Phys. Chem. C* **2016**, *120*, 14345−14355.
(34) Kohn, W.; Sham, L. J. Self-Consistent Equations Including Exchange and Correlation Effects. *Phys. Rev.* **1965**, *140*, A1133−A1138.
(35) Perdew, J. P.; Burke, K.; Ernzerhof, M. Generalized Gradient Approximation Made Simple. *Phys. Rev. Lett.* **1996**, *77*, 3865−3868.
(36) Blöchl, P. E. Projector Augmented-Wave Method. *Phys. Rev. B: Condens. Matter Mater. Phys.* **1994**, *50*, 17953−17979.
(37) Kresse, G.; Joubert, D. From Ultrasoft Pseudopotentials to the Projector Augmented-wave Method. *Phys. Rev. B: Condens. Matter Mater. Phys.* **1999**, *59*, 1758−1775.
(38) Grimme, S. Semiempirical GGA-Type Density Functional Constructed with a Long-Range Dispersion Correction. *J. Comput. Chem.* **2006**, *27*, 1787−1799.
(39) Ataca, C.; Topsakal, M.; Aktürk, E.; Ciraci, S. A Comparative Study of Lattice Dynamics of Three- and Two-Dimensional MoS_2. *J. Phys. Chem. C* **2011**, *115*, 16354−16361.
(40) Praveen, C. S.; Piccinin, S.; Fabris, S. Adsorption of Alkali Adatoms on Graphene Supported by the Au/Ni(111) Surface. *Phys. Rev. B: Condens. Matter Mater. Phys.* **2015**, *92*, 075403.
(41) Dion, M.; Rydberg, H.; Schroder, E.; Langreth, D.; Lundqvist, B. I. *Phys. Rev. Lett.* **2004**, *92*, 246401.
(42) Monkhorst, H. J.; Pack, J. D. Special Points for Brillouin-Zone Integrations. *Phys. Rev. B* **1976**, *13*, 5188−5192.
(43) Kresse, G.; Furthmüller, J. Efficient Iterative Schemes for Ab Initio Total-Energy Calculations Using a Plane-Wave Basis Set. *Phys. Rev. B: Condens. Matter Mater. Phys.* **1996**, *54*, 11169−11186.
(44) Kresse, G.; Furthmüller, J. Efficiency of Ab-initio Total Energy Calculations for Metals and Semiconductors Using a Plane-wave Basis Set. *Comput. Mater. Sci.* **1996**, *6*, 15−50.
(45) Gillan, M. J. Calculation of Vacancy Formation Energy in Aluminum. *J. Phys.: Condens. Matter* **1989**, *1*, 689.

DOI: 10.1021/acs.jpcc.6b11705
J. Phys. Chem. C 2017, 121, 6329−6338

(46) Heyd, J.; Scuseria, G. E.; Ernzerhof, M. Hybrid Functionals Based on a Screened Coulomb Potential. *J. Chem. Phys.* **2003**, *118*, 8207.
(47) Heyd, J.; Scuseria, G. E.; Ernzerhof, M. Erratum: 'Hybrid Functionals Based on a Screened Coulomb Potential' [J. Chem. Phys. 118, 8207 (2003)]. *J. Chem. Phys.* **2006**, *124*, 219906.
(48) Topsakal, M.; Şahin, H.; Ciraci, S. Graphene Coatings: An Efficient Protection from Oxidation. *Phys. Rev. B: Condens. Matter Mater. Phys.* **2012**, *85*, 155445.

DOI: 10.1021/acs.jpcc.6b11705
J. Phys. Chem. C 2017, 121, 6329−6338